

RESEARCH ARTICLE

Determination of the damping ratio of the Yusufeli Arch Dam under low-magnitude earthquakes during operational conditions

Fatih Yesevi Okur^{1,2*}

- ¹ Karadeniz Technical University, Department of Civil Engineering, 61080, Trabzon, Türkiye
- ² Earthquake and Structural Health Monitoring Research Center, Karadeniz Technical University, 61080, Trabzon, Türkiye

Article History

Received 14 July 2025 Accepted 15 September 2025

Keywords

Arch dam
Damping ratio
Logarithmic decrement
Low-intensity earthquake
Reservoir effect
Seismic behavior
Structural health monitoring

Abstract

Concrete arch dams rely on energy dissipation through material damping and boundary interactions to attenuate seismic vibrations, yet quantitative field measurements of damping under real operating conditions are scarce. In this study, we present a comprehensive damping assessment of the 275 m-high Yusufeli Arch Dam during its reservoir impoundment phase (2022-2025). Six low-magnitude earthquakes (Mw 4.0-5.0) provided crest-level acceleration records via a centrally located tri-axial sensor. A multi-band logarithmic-decrement technique was employed, with filter frequencies adjusted according to real-time water-leveldependent natural frequencies. The resulting damping ratios ranged from 0.8% to 4.7% (mean 1.95%, COV 23%), revealing a strong amplitude dependence: higher crest peak accelerations corresponded to increased damping, while no clear trend emerged with reservoir fill level. These results demonstrate that under service-level seismic inputs, a constant damping ratio of 1-2% can be reliably assumed across impoundment stages, with higher values only necessary for stronger shaking. The methodology's reliance on a single, easily maintained sensor and direct response data offers a practical approach for structural health monitoring and model calibration. By decoupling damping from continuous hydraulic loading variations and focusing on measured excitation amplitude, this framework enhances the accuracy of seismic response simulations and supports more effective maintenance and risk-mitigation strategies for large arch dams.

1. Introduction

In recent years, the number and size of large dams worldwide have increased rapidly; according to data from the International Commission on Large Dams (ICOLD), there are now over 60,000 large dams globally [1]. These massive structures provide significant benefits in terms of energy production, flood control, and water supply, yet they also pose substantial risks to their surrounding environments. Particularly, concrete arch dams are susceptible to physical, chemical, and structural effects throughout their long service lives, leading to potential variations in performance and safety levels [1]. Therefore, close monitoring of their structural behavior through reliable and continuous methods has become an engineering necessity.

eISSN 2630-5763 © 2023 Authors. Publishing services by golden light publishing®.

^{*} Corresponding author (yesevi@ktu.edu.tr)

Okur Okur

The dynamic characteristics of dams, such as natural frequencies, mode shapes, and damping ratios, play a critical role in determining their response to dynamic loads like earthquakes and are essential for structural health monitoring (SHM) [2]. Changes in these modal parameters over time can reflect damage or stiffness loss in the dam body; hence, long-term modal analysis provides valuable insight into the dam's structural condition. However, it is now well understood that environmental and operational conditions can also significantly affect these modal parameters, leading to observable variations in frequency and damping even in the absence of physical damage [2]. Several studies have confirmed that modal properties of dams are strongly influenced by external factors such as temperature and reservoir water level, and that observed deviations in SHM data cannot always be attributed to damage alone [1].

One of the most critical parameters for understanding seismic behavior is the modal damping ratio, which quantifies a structure's ability to dissipate vibrational energy. Damping plays a fundamental role in dam safety and performance as it directly controls the dissipation of seismic energy. Accurate estimation of damping ratios is essential for realistic seismic simulations, structural health monitoring, and the calibration of finite element models. Underestimation may result in over-conservative safety margins, while overestimation may underestimate seismic demands, potentially compromising risk assessments. While fixed damping ratios (e.g., 5%) are often assumed in engineering design for simplicity [3], the actual damping behavior of large concrete dams can deviate significantly from these nominal values. Laboratory tests and ambient vibration studies typically report concrete material damping ratios below 2%, whereas damping ratios derived from strong earthquake records can range as high as 8-15% [4]. In various arch dams, the firstmode damping ratios under small vibration amplitudes are often observed in the range of 2-4%, but significantly increase with seismic acceleration due to nonlinear effects such as stress softening, joint openings, and foundation-soil interactions [4]. In well-known dams such as Fei-Tsui, Emosson, and Mauvoisin, damping ratios below 4% were found in forced vibration tests, while ratios up to 15% were calculated during strong seismic events. These findings confirm that damping is a complex, amplitudedependent structural property and that additional energy dissipation mechanisms become active as vibration intensity increases [4].

Recent studies using real earthquake recordings from Turkey's major seismic events, such as the February 2023 Kahramanmaraş earthquakes, also indicate that effective damping ratios can exceed design expectations. Analysis of acceleration data from several undamaged dams revealed that peak damping values ranged between 7–11%, with values as high as 10% at the crest of Tahtaköprü earthfill dam and 8% for rockfill dams like Kavşak Bendi [5]. These values significantly exceed the conventional 5% design assumption, demonstrating the potential for higher damping capacity even under moderate excitations.

Environmental factors such as reservoir water level and air temperature are also known to influence the dynamic behavior of concrete dams [1, 6]. Typically, an increase in water level adds mass and alters the effective stiffness of the dam–reservoir system, causing a decrease in modal frequencies. Temperature changes, on the other hand, affect concrete stiffness through thermal expansion and internal stress gradients [1]. Long-term SHM studies have confirmed that the first natural frequency of dams often varies inversely with reservoir water level, while higher modes are more sensitive to daily temperature fluctuations [6]. Regression-based modeling of these environmental effects has been shown to reduce the scatter in modal frequency estimation by over 50%, enabling better isolation of structural anomalies from environmental influences [1]. In contrast, the extent to which environmental conditions affect modal damping ratios remains poorly understood. While some long-term studies report high variability in damping estimates and weak correlation with water level or temperature [1], others point to methodological uncertainties such as low signal-to-noise ratio in ambient signals and limitations in OMA algorithms as the source of inconsistency [1]. Moreover, the energy dissipation mechanisms in dams (e.g., internal material damping, friction in structural connections, radiation damping to the foundation) are not as directly affected by environmental

variables as modal frequencies [2]. As a result, the influence of environmental conditions on damping remains a debated and understudied topic in the literature.

Concrete arch dams, distinguished by their slender double-curvature geometry and reliance on arch action to transfer loads to the abutments, tend to exhibit lower inherent damping than gravity or rockfill dams; field measurements commonly report first-mode damping ratios between ~0.3 % and 4 % under low-amplitude excitation [7-9]. Full-scale forced-vibration tests on Monticello Dam in California showed modal damping clustered around 2–3 %, whereas ambient-vibration studies on Türkiye's 201 m-high Berke Dam revealed values as low as 0.6 % [8]. More recent campaigns that combined operational modal analysis with controlled shakers such as the nine-mode identification of Shahid Rajaee Dam (138 m) and the long-term ambient/earthquake monitoring of Karun IV Dam (230 m) confirmed that damping increases modestly with vibration amplitude, rising to 3–5 % for small earthquakes but remaining well below the conventional 5 % design assumption [9, 10]. Experimental evidence further indicates that reservoir water level and foundation radiation make only secondary contributions to damping, while temperature effects are largely confined to modal frequencies [11, 12]. Collectively, these studies highlight the amplitude-dependent and site-specific nature of damping in high concrete arch dams and underscore the importance of continuous, in-situ monitoring to capture subtle temporal trends that could signify stiffness degradation or incipient damage.

Despite the growing body of work on dam dynamics and environmental influence, there is a significant research gap concerning the long-term evolution of damping ratios under low-level earthquake excitations in high arch dams. Most existing studies focus on either ambient vibration testing or high-intensity seismic events and rarely provide time-resolved damping trends over extended monitoring periods. Moreover, the combined effect of reservoir water level on damping behavior has not been systematically analyzed, and the available findings remain sparse and inconclusive. Some researchers report negligible influence of environmental factors on damping, while others suggest possible indirect effects, but no generalizable model or consensus has yet been reached [1].

To address this critical gap, the primary objective of this study is to quantify and interpret the damping behavior of the Yusufeli Arch Dam, Türkiye's tallest dam (275 m high), during its reservoir impoundment stage using low-magnitude earthquake records. In particular, the study aims to clarify how damping ratios evolve in the elastic response range and to provide practical, amplitude-dependent values that can be directly applied in structural health monitoring systems and numerical seismic response simulations. In this study, we selected a set of low-magnitude earthquake events and applied the logarithmic decrement method to calculate the damping ratios from free-vibration decay segments. The influence of reservoir water level was statistically analyzed to assess its impact on damping variability. The results provide a comprehensive assessment of damping behavior under operational conditions and offer new insights into the environmental dependencies of damping in high concrete arch dams. Based on the existing literature and monitoring data, this study aims to demonstrate that damping ratios of the Yusufeli Arch Dam remain in the 1-2% range under low-magnitude earthquakes, independent of reservoir level, while increasing with excitation amplitude. The expected outcome is to provide practical, amplitude-dependent damping values that can be directly applied in seismic safety assessments, SHM systems, and numerical model calibration. This work fills a crucial gap in the literature and contributes valuable data for improving seismic safety evaluations and SHM practices in large dam structures.

2. State-of-the-art on damping ratios in concrete arch dams

Concrete arch dams have been the subject of dynamic testing for almost six decades, yet a consolidated picture of their damping behavior has only started to emerge in the past ten years. Early knowledge was shaped by large-scale forced-vibration campaigns on U.S. prototypes such as Monticello and Morrow Point. Using twin electromechanical shakers (\approx 22 kN each), Clough et.al. [7] identified the first few modes of

Monticello Dam and reported damping ratios clustered around 2-3 % for low-amplitude (elastic) response, establishing the first reliable benchmark for a full-reservoir arch dam. Similar amplitudes were found in subsequent tests on Morrow Point Dam, confirming that material damping alone is well below the 5 % design norm.

With the advent of high-sensitivity accelerometers and output-only identification algorithms, the research focus migrated to Operational Modal Analysis (OMA). Ambient-vibration measurements on the 201 m-high Berke Dam (Türkiye) delivered a first-mode damping of only 0.6%, illustrating how truly free-field excitation isolates material damping when radiation losses are small [8]. Continuous ambient monitoring of the 250 m-high Mauvoisin Dam revealed that water-level variations modify frequencies by up to 7% but affect damping only marginally; first-mode values remained below 3 % throughout a full hydrological cycle [11, 13]. More recently, automated SSI-COV pipelines have been run for a full year on Baixo Sabor Dam (Portugal), enabling unsupervised tracking of the first four modes and confirming a steady-state damping envelope of 1–2% under normal operation [12, 14]. Such long records have also highlighted the need to filter out temperature-induced bias before attributing fluctuations to damage [1, 12].

Recognizing that amplitude dependence is still poorly captured by ambient data alone, a new generation of hybrid campaigns combines controlled exciters with OMA. The first full-scale experiment of this kind was carried out on Iran's Shahid Rajaee Dam (138 m): nine modes up to 14 Hz were extracted, and damping ratios rose from \approx 1% at shaker-on/off levels to \approx 4% under swept-sine loading, demonstrating a clear but moderate amplitude effect [9]. A follow-up study on the 230 m-high Karun IV Dam merged one year of ambient data with low-magnitude earthquake records; first-mode damping increased from \approx 3% (ambient) to \approx 5% (PGA \approx 0.03g), while higher modes showed proportionally smaller growth [10]. These results corroborate observations from historic earthquake recordings at Pacoima and Emosson dams, where strong shaking (> 0.3g) activated additional dissipation mechanisms and pushed damping into the 8–15% range [11].

Research into environmental and boundary effects has refined the physical interpretation of these numbers. Analytical–experimental studies on Mauvoisin demonstrated that reservoir-induced radiation contributes roughly 0.5–1% to global damping, whereas temperature mainly shifts stiffness and leaves damping nearly unchanged [15]. Numerical parametric work confirms that foundation radiation becomes comparable with material damping only for the first two modes, explaining why higher-order modes tend to settle below 2% even in deep valleys [15].

Automation and big data perspectives have emerged as a separate research front. Recent machine-learning pipelines for Baixo Sabor and Portuguese multi-dam portfolios apply clustering and causal filtering to tens of thousands of OMA runs, achieving sub-0.1% uncertainty in modal damping estimates and enabling near-real-time anomaly detection [12, 16]. Parallel advances in balanced stochastic subspace identification promise robust extraction of lightly damped modes ($\zeta < 1\%$) in noise-dominated data, as demonstrated on Shahid Rajaee and Karun IV archives [17, 18].

Despite these advances, several important gaps persist in the current understanding of damping behavior in high arch dams, particularly under realistic operational scenarios. Most existing studies focus either on short-term ambient vibration records or on isolated seismic events, with limited attention to how damping ratios evolve during long-term reservoir filling or drawdown cycles. As a result, the combined influence of reservoir water level and earthquake-induced excitation on damping remains largely unquantified, especially in tall arch dams transitioning from empty to full conditions. While frequency variations due to hydrodynamic mass and temperature gradients are well documented, the corresponding changes in modal damping across different water levels are rarely addressed in a systematic, time-resolved manner. In particular, there is a lack of studies analyzing low-magnitude seismic events (e.g., PGA < 0.05g) across multiple reservoir stages to assess how energy dissipation mechanisms may shift due to hydrostatic pressure,

joint activation, or foundation–reservoir interactions. Furthermore, few works employ high-resolution instrumentation capable of isolating free-decay responses under such subtle loading conditions. Consequently, current models cannot reliably predict how damping evolves during a dam's transition from dry to impounded states—posing a limitation for both safety evaluations and SHM algorithms. The present study directly addresses this gap by investigating the damping behavior of a concrete arch dam across varying water levels using long-term SHM data and low-level seismic records.

3. Description of the Yusufeli Arch Dam and instrumentation

The Yusufeli Arch Dam, located in the northeastern region of Türkiye on the Çoruh River in Artvin Province, stands as the tallest dam in the country and one of the highest double-curvature concrete arch dams in the world. Rising 275 meters from its foundation to the crest elevation of +715 meters, it is a flagship component of Türkiye's hydroelectric development strategy and a cornerstone of the Çoruh River Hydroelectric Master Plan. The dam was constructed between 2013 and 2022, and impoundment operations began in late 2022. Power generation commenced in November 2023, with an installed capacity of 540 MW and an expected annual output of 1.8 billion kWh. In addition to electricity generation, the dam plays a key role in regional flood control and irrigation, supported by its capacity to store up to 270 million cubic meters of water.

The dam's structural design features a double-curved geometry that allows hydrostatic forces to be transferred efficiently to the abutments. This geometry, along with its slender cross-section and massive scale, makes it highly sensitive to dynamic loads such as earthquakes and reservoir-induced vibrations. Due to this sensitivity, real-time structural monitoring under operational conditions is essential for assessing the dam's dynamic behavior and ensuring long-term safety. Fig. 1 provides general views of the Yusufeli Arch Dam and the surrounding topography.



Fig. 1. The views of Yusufeli Arch Dam [19]

Due to its high elevation, double-curved geometry, and slender cross-section, the Yusufeli Arch Dam exhibits a highly sensitive dynamic behavior under environmental and seismic excitations. This sensitivity necessitates a reliable SHM system capable of continuously observing the dam's dynamic response under operational conditions. In response to this need, a focused instrumentation strategy was developed, aiming to capture essential dynamic behavior with a minimal number of high-precision sensors. The approach centers on long-term monitoring through permanent instrumentation located along the dam crest, where vibration amplitudes tend to be most pronounced.

The SHM system utilizes three high-sensitivity tri-axial accelerometers (Sara SL06) with a dynamic range of 156 dB and a frequency bandwidth spanning 0 to 1500 Hz. These accelerometers were selected for their robustness, accuracy, and suitability for low-amplitude vibration detection under real field conditions. The installation layout was designed to leverage the symmetrical nature of the dam's modal response. One accelerometer was placed precisely at the geometric midpoint of the dam crest, serving as the main reference sensor, while the other two were installed symmetrically on either side, spaced approximately 82 meters from the center. This configuration enables effective coverage of the crest while minimizing complexity in wiring and data acquisition. Although three sensors were deployed, the current study specifically focuses on the data obtained from the centrally located accelerometer, which is considered to be sufficiently representative of the dam's global vibrational behavior, especially for low-intensity dynamic events such as small-magnitude earthquakes.

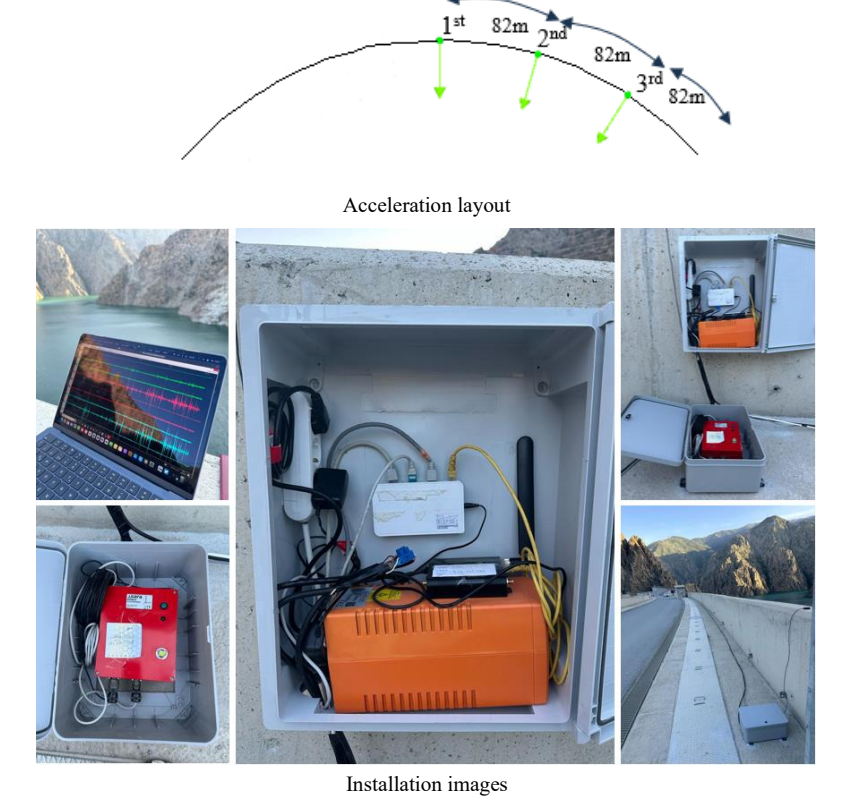


Fig. 2. Installation views and configuration of crest-mounted accelerometers during the reservoir impoundment stage [19]

Each accelerometer is connected via shielded Ethernet cables to a nearby monitoring cabinet that houses the data acquisition infrastructure. This includes an industrial-grade 3G modem for data transmission, a programmable signal switching module for remote sensor control, and an uninterruptible power supply (UPS) to ensure continued operation in the event of power loss. A GSM-based communication system using a SIM card with a monthly 100 GB data allowance was integrated to facilitate reliable real-time data transfer. The data collected from the midpoint sensor are transmitted periodically to a secure remote server, allowing long-term storage, remote access, and detailed post-processing. The layout and field deployment of the three accelerometers along the dam crest are illustrated in Fig. 2.

The system is designed for autonomous operation and remote management. Sensors can be activated or deactivated based on scheduled routines or external triggers, such as detected seismic activity. The signal switching mechanism also allows the system to be reset or reconfigured remotely in case of data loss or communication faults. Thanks to the robust power and network setup, the Yusufeli Dam monitoring infrastructure has proven resilient throughout varying environmental conditions and across all stages of reservoir filling—from the initial empty state to near-full impoundment.

This targeted and efficient instrumentation scheme reflects a modern approach to SHM in large-scale civil infrastructure. By focusing on high-quality data acquisition at strategically chosen points, especially the crest midpoint where structural response is most significant, it becomes possible to track critical changes in dynamic behavior with minimal equipment. The configuration used at Yusufeli Arch Dam ensures reliable monitoring performance over extended timeframes, supporting data-driven safety assessments and providing valuable input for future engineering analyses.

4. Selected earthquake events and data characteristics

This study focuses on six low-magnitude earthquake events that occurred during the operational phase of the Yusufeli Arch Dam, specifically throughout the reservoir impoundment period. These events were selected based on their suitability for evaluating the dam's vibrational response under low-amplitude dynamic loading, which is particularly relevant for assessing damping behavior in the elastic range. All acceleration data used in the analysis were obtained from the tri-axial accelerometer installed at the geometric center of the dam crest, which that chosen for its strategic position to capture global structural response characteristics.

The selected earthquakes span a range of dates between 09.27.2022 – 01.08.2025, covering different stages of reservoir filling from initial impoundment to near-full capacity. This temporal distribution provides a valuable opportunity to examine how structural response parameters evolve as hydrostatic loading increases. While the primary aim of this study is not to investigate the direct effect of water level, the inclusion of events from varying reservoir conditions offers context for interpreting damping variability across operational scenarios.

Basic preprocessing steps were applied to each signal to ensure consistency across the dataset. These included detrending, baseline correction, and band-pass filtering, typically in the range of 0.05 Hz to 25 Hz to remove low-frequency drift and high-frequency noise. Only those records exhibiting clear transient vibrations attributable to seismic excitation were retained for subsequent damping analysis.

A summary of the six selected events is presented in Table 1. The table includes the date and time of each earthquake, magnitude, epicentral distance, and the peak acceleration values recorded at the crest of the Yusufeli Arch Dam. Since no accelerometer is installed at the dam foundation, conventional peak ground acceleration (PGA) values could not be directly measured. Instead, the recorded peak acceleration at the crest-level sensor was used as a representative indicator of the dam's dynamic excitation. These crest peak acceleration (CPA) values reflect the structural response under each seismic event and form the basis for damping assessment in this study. Although not equivalent to true ground motion input, they provide

consistent and reliable excitation levels for comparative analysis, particularly under low-amplitude conditions.

The recorded CPA, ranging approximately from 0.00017 - 0.04332g, confirms that all events fall within the elastic response regime, making them suitable for evaluating the dam's damping behavior without the confounding influence of inelastic deformation or structural damage. Time-history acceleration recordings obtained at the dam crest for all six selected earthquake events are presented in Fig. 3, providing a comparative view of the vibrational response under varying excitation levels.

These earthquake records serve as the basis for all damping estimations presented in this study. Their diversity in both seismic and reservoir parameters allows for a more detailed interpretation of the dam's dynamic behavior under realistic operational conditions. By focusing on consistent measurement conditions and well-documented events, this dataset supports a controlled analysis of damping trends that are both representative and methodologically sound.

Table 1. Summary of the six selected earthquake events, including date, magnitude, epicentral distance, and crest-recorded peak acceleration values

No	Location	Datetime (UTC)	Distance to Dam (km)	Magnitude (Mw)	CPA (%g)
1	Göle (Ardahan)	27-09-2022 14:03	107	5.0	0.0535
2	Aziziye (Erzurum)	11-06-2023 07:41	92	4.6	0.0642
3	Narman (Erzurum)	01-08-2023 18:37	78	4.1	0.1555
4	Hemşin (Rize)	15-11-2024 09:02	58	4.7	4.3323
5	Kağızman (Kars)	24-11-2024 01:47	144	4.0	0.0172
6	Pasinler (Erzurum)	08-01-2025 01:30	106	4.5	0.1599

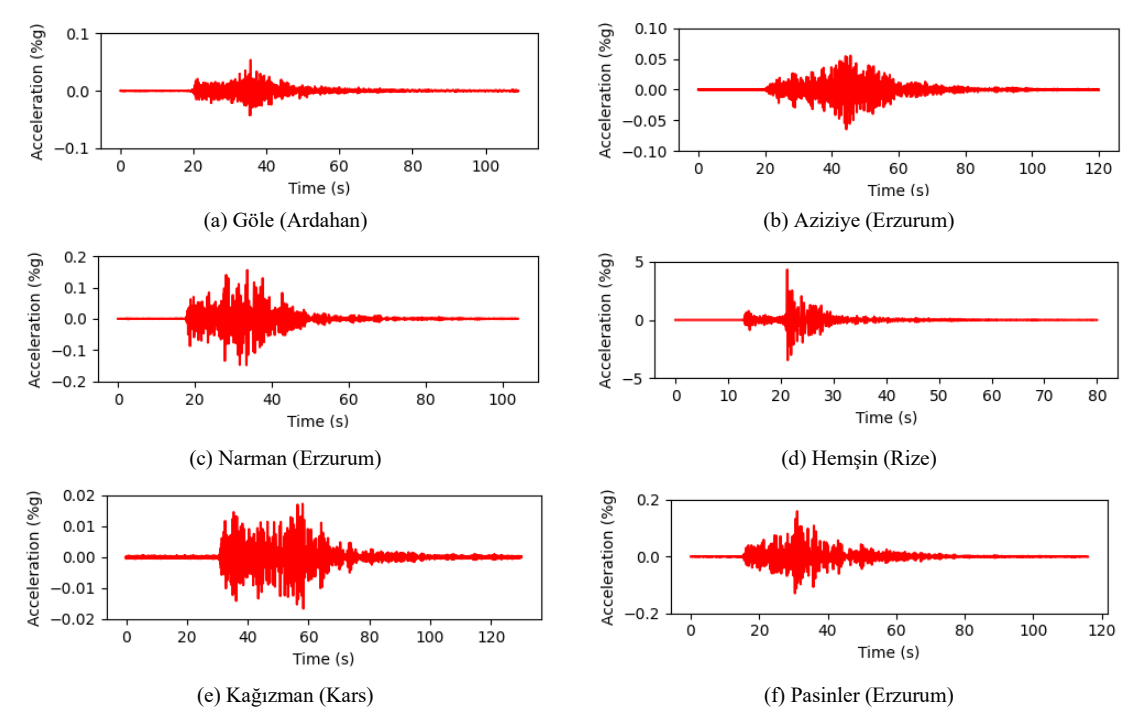


Fig. 3. Time-history acceleration records measured at the dam crest for the six selected earthquake events

5. Methodology for damping estimation

The damping ratio of the Yusufeli Arch Dam was derived from the crest-level earthquake records by applying a three-step workflow (signal pre-processing, free-decay extraction, and logarithmic-decrement calculation) commonly recommended for large civil structures when only response data are available [20, 21]. Each three-component accelerogram was first detrended and baseline-corrected with a third-order polynomial, then filtered with a zero-phase fourth-order Butterworth band-pass (0.5–25 Hz) to suppress low-frequency drift and high-frequency sensor noise. This pass-band encompasses the dominant modal content of tall arch dams and follows the ranges employed in previous crest-only studies [4, 8]. Only the upstream–downstream component—consistently the most energetic—was retained for analysis.

For every earthquake, the absolute-maximum acceleration instant was identified, and a free-decay segment was extracted starting 0.5 s after this peak and ending when the signal amplitude dropped below 2 % of its maximum. Such a short time lag minimizes the influence of ongoing ground motion and improves the reliability of damping estimates based on single-point data [20]. The extracted segment was then narrowband filtered around the dam's dominant natural frequency with a bandwidth of ± 0.3 Hz, an approach shown to reduce modal interaction errors in lightly damped systems [22]. Successive positive peaks were automatically detected, and the logarithmic decrement as

$$\delta = \frac{1}{j} \ln \left(\frac{u_1}{u_{j+1}} \right) \tag{1}$$

was computed over j cycles. The damping ratio was obtained from

$$\zeta = \frac{\delta}{\sqrt{\delta^2 + 4\pi^2}} \tag{2}$$

The logarithmic-decrement method is preferred here because it quantifies energy dissipation directly from free decay, requires only a single response channel, and has been validated for large concrete dams subjected to weak seismic input [8, 20]. Although frequency-domain techniques such as half-power bandwidth or EFDD are available, they are less robust under the single-sensor, lightly damped conditions encountered in this study [4]. Accordingly, this study relies exclusively on the logarithmic-decrement approach, and this technique enables us to quantify the damping of the Yusufeli Arch Dam accurately from a single crest-sensor record within the elastic response range.

6. Results and discussion

Crest-level recordings from the six low-magnitude earthquakes were processed with the multi-band logarithmic-decrement workflow described in Section 5. For each event, the band-pass filter was centered on the first-mode frequency obtained by the water-level—frequency curve of Kalkan Okur [19], ensuring that every free-decay segment corresponded to the same structural mode despite the continuously rising reservoir. This alignment eliminates modal leakage and makes the resulting damping ratios directly comparable across different impoundment stages.

Fig. 4 presents the crest-recorded displacement time series for the six earthquakes analyzed in this study. In each trace, the entire response is shown in light grey, while the pale-yellow band marks the free-decay portion automatically selected for damping evaluation. The corresponding narrow-band filtered signal, centered on the water-level-dependent first-mode frequency, is superimposed in blue. The red curve is the least-squares exponential envelope fitted to those peaks; the damping ratio obtained from that envelope is reported in the title of each sub-figure.

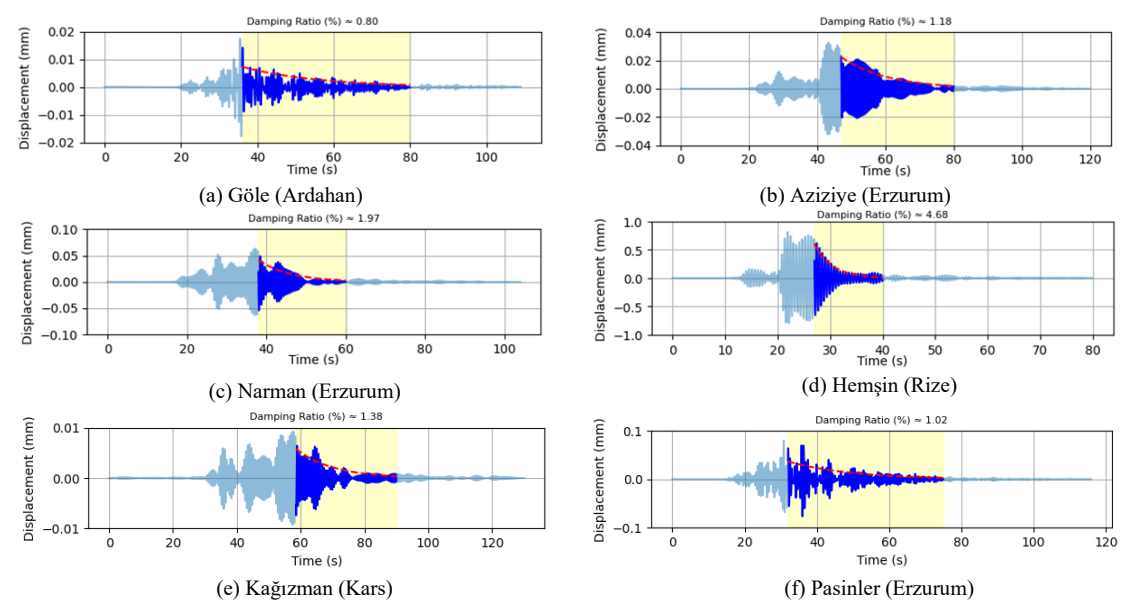


Fig. 4. Narrow-band free-decay responses for six earthquakes: filtered displacement (blue) and fitted logarithmic envelopes (red)

Table 2. Summary of crest-recorded peak acceleration, reservoir water level, water-level-dependent natural frequency, and calculated damping ratio for the six selected earthquake events

No	Location	Damping Ratio (%)	CPA (%g)	Frequency (Hz)	Water-Level (m)
1	Göle (Ardahan)	0.80	0.0535	1.88	0
2	Aziziye (Erzurum)	1.18	0.0642	1.86	158
3	Narman (Erzurum)	1.97	0.1555	1.76	180
4	Hemşin (Rize)	4.68	4.3323	1.81	185
5	Kağızman (Kars)	1.38	0.0172	1.81	185
6	Pasinler (Erzurum)	1.02	0.1599	1.95	175

Table 2 provides a comprehensive summary of the quantitative results derived from the damping analysis of all six earthquake events. For each record, the table reports the date of occurrence, reservoir water level at the time of the event, the corresponding first-mode natural frequency used for filtering (as estimated from the water level–frequency relationship measurement by Kalkan Okur [19], the CPA, and the calculated damping ratio. CPA recorded during the six selected low-magnitude earthquakes yielded damping ratios between 0.80% and 4.68%, despite CPA varying from 0.017g to 0.160g (Table 2). The minimum damping of 0.80% was observed at Göle when the reservoir was empty (0 m; f = 1.88 Hz, CPA = 0.0535g), while the maximum of 4.68% occurred at Hemşin under near-full impoundment (185 m; f = 1.81 Hz, CPA = 4.3323g). Intermediate events at Aziziye (158 m; f = 1.86 Hz, $\zeta = 1.18\%$, CPA = 0.0642 g), Narman (180 m; f = 1.76 Hz, $\zeta = 1.97\%$, CPA = 0.1553 g) and Pasinler (175 m; f = 1.95 Hz, Damping ratio = 1.02%, CPA = 0.1599 g) produced damping values in the 1–2% range. Overall, the mean damping ratio across all events is 1.95%, with a coefficient of variation of 23%.

The scatter distribution in Fig. 5 underscores a clear amplitude dependence of damping in the Yusufeli Arch Dam: as CPA increases from 0.017g to 0.159g, the damping ratio climbs steadily from roughly 1% to nearly 2% for most events. This trend aligns with laboratory and field observations that microcracking, friction at construction joints, and interface slipping become more active as cyclic strain amplitudes rise [4]. It also mirrors findings from forced-vibration tests on arch dams, where the damping ratio grew from 1% at low amplitudes to 4–5% under stronger shaker inputs [9].

By contrast, reservoir water level encoded as marker size in Fig. 5 exerts no consistent influence on damping ratio. Events at the same water level (e.g., Kağızman and Hemşin, both at 185 m) yield dramatically different damping ratios (1.4% vs. 4.7%), whereas events separated by 25 m of head (Aziziye at 158 m and Narman at 180 m) show damping ratio values within the same band (1.2–2%). This decoupling of damping ratio from hydrostatic loading confirms that, under elastic-range excitations, added water mass and fluid-structure interaction primarily shift natural frequencies rather than alter energy-dissipation mechanisms [11, 12].

The pronounced outlier at Hemşin (Damping ratio= 4.68%, CPA = 0.043g) is consistent with the well-documented amplitude dependence of damping, whereby higher excitation levels activate additional energy-dissipation mechanisms such as microcracking and joint friction [4]. Evaluating whether this elevated damping persists across similar high-CPA events would clarify whether it represented a systematic nonlinear response or an isolated measurement anomaly.

Taken together, these results hold direct implications for both SHM and numerical modeling of large arch dams. For low-amplitude, service-level excitations (CPA < 0.05g), a nominal damping ratio of $\sim 1-2\%$ is sufficient and can be applied universally across water levels. For stronger motions (CPA > 0.1g), a graduated increase in damping ratio guided by the trend line of Fig. 5 should be incorporated into seismic response simulations to capture nonlinear dissipation. This strategy simplifies SHM algorithms by decoupling damping from continuously varying reservoir levels, instead focusing on real-time measurement of CPA and local boundary conditions.

Nevertheless, the present study is limited by its reliance on a single crest sensor and a relatively small event set. Future work should extend the analysis to include multi-point arrays, enabling spatial mapping of damping heterogeneity, and larger catalogs of small-to-moderate quakes to refine the damping ratio, CPA, and water-level calibration curve. Additionally, controlled low-amplitude shaker tests at selected water levels would help isolate the pure hydrostatic contribution to damping, further improving predictive models for dam safety assessments.

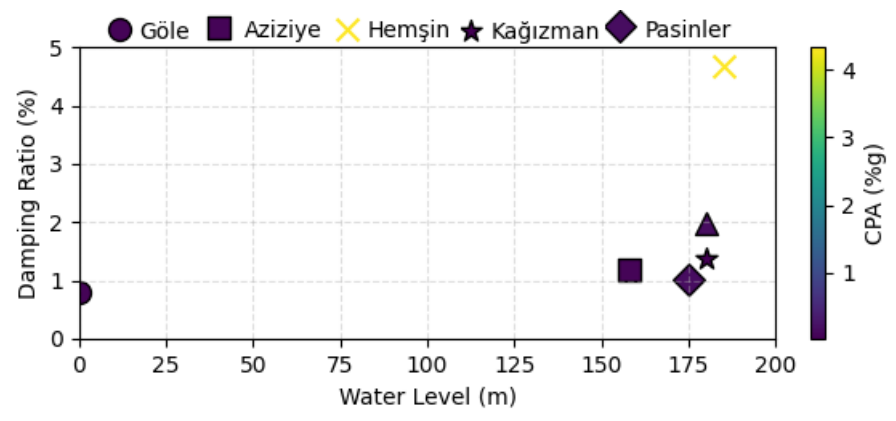


Fig. 5. Comparison of water level versus damping ratio, with marker size proportional to CPA

7. Conclusions

The present study has quantified the damping behavior of the Yusufeli Arch Dam under six low-magnitude earthquake events recorded during the reservoir impoundment phase. By applying a consistent, single-sensor, multi-band logarithmic-decrement method with filter frequencies tied to the water-level-frequency relationship of Kalkan Okur [19], we obtained damping ratios ranging from 0.80% to 4.68%, with a mean of 1.95% and a coefficient of variation of 23 %. These values fall within the 1–3% window commonly reported for arch dams under low-amplitude excitation and confirm the dam's stable energy-dissipation capacity across markedly different hydrodynamic and seismic loading conditions.

A clear positive correlation was observed between CPA and damping ratio, indicating that higher excitation amplitudes activate nonlinear dissipation mechanisms such as microcracking and joint friction. In contrast, changes in reservoir water level exerted no systematic influence on damping, suggesting that hydrostatic loading primarily shifts natural frequency without modifying core energy-dissipation processes. The pronounced outlier at Hemşin (Damping ratio = 4.68% at CPA = 0.043g) is consistent with this amplitude dependence and highlights the need to account for localized structural or boundary conditions when interpreting extreme values.

From a practical standpoint, these findings support the use of a single, water-level-independent damping ratio of approximately 1-2% for service-level seismic monitoring and numerical modeling of the Yusufeli Arch Dam. For stronger excitations (CPA > 0.1g), models should incorporate an amplitude-dependent increase in damping ratio to capture nonlinear dissipation accurately. This approach simplifies SHM algorithms by decoupling damping from continuously varying reservoir levels and focusing instead on real-time measurement of crest acceleration and known boundary conditions.

Building on the findings of this study, future research should pursue several complementary avenues to deepen our understanding of damping behavior in large arch dams. First, deploying a spatially distributed array of accelerometers across the dam crest and abutments will illuminate the heterogeneity of energy dissipation, enabling identification of localized hotspots of microcracking or joint friction under varying excitation amplitudes. Second, expanding the earthquake catalogue to include a larger number of small-to-moderate events will refine the statistical relationship between crest peak acceleration and damping ratio, improving confidence in the amplitude-dependent calibration and helping to distinguish systematic nonlinear effects from isolated anomalies. Finally, controlled shaker tests conducted at selected water levels would isolate the pure hydrostatic contribution to damping, allowing a direct quantification of fluid–structure interaction effects without confounding seismic input. Integrating these empirically derived, amplitude- and water-level–dependent damping values into detailed finite-element models of the dam–reservoir–foundation system will further enhance seismic response predictions and risk assessments.

Overall, this study demonstrates that damping ratios of the Yusufeli Arch Dam remain stable at approximately 1–2% under low-magnitude earthquakes, independent of reservoir level, while increasing with excitation amplitude. This clear trend provides a practical take-home message for seismic modeling and SHM applications, ensuring more realistic and reliable safety assessments.

Acknowledgements

The author would like to thank the General Directorate of State Hydraulic Works (DSİ) for their support and cooperation in data collection at the Yusufeli Arch Dam. Without DSİ's permission and logistical assistance, this study would not have been possible.

Declaration of conflicting interests

The author(s) declared no potential conflicts of interest with respect to the research, authorship, and/or publication of this article.

Funding

No funding was received for this study.

Data availability statement

The crest-level acceleration and seismic event data that support the findings of this study are owned by DSİ. These data can be made available to qualified researchers upon reasonable request and with prior written approval from DSİ.

References

- [1] Ardila-Ardila YV, Gómez-Araújo ID, Villalba-Morales JD, Aracayo LA (2025) Effect of environmental factors on modal identification of a hydroelectric dam's hollow-gravity concrete block. J Civil Struct Health Monit 15(3):777-794.
- [2] Qu C, Tu G, Gao F, Sun L, Pan S, Chen D (2024) Review of bridge structure damping model and identification method. Sustainability 16(21):9410.
- [3] Wang F, Yang Z, Song Z, Liu Y, Tan Y, Liu X (2024) Influence of SV wave oblique incidence on the dynamic response of arch dams under canyon contraction. Water 16(24):3630.
- [4] Cheng L, Ma C, Yuan X, Yang J, Hu L, Zheng D (2022) A literature review and result interpretation of the system identification of arch dams using seismic monitoring data. Water 14(20):3207.
- [5] Bayraktar A, Akköse M, Ventura CE, Yang TY, Hökelekli E (2024) Onsite seismic monitoring behavior of undamaged dams during the 2023 Kahramanmaraş earthquakes (M7.7 and M7.6). Sensors 24(21):6856.
- [6] Cunha A, Pereira S, Gomes J, Magalhães F, Lemos JV (2023) Seven years of continuous dynamic monitoring of Baixo Sabor Dam. In: Proc 9th ECCOMAS Thematic Conf on Computational Methods in Structural Dynamics and Earthquake Engineering, Athens, Greece.
- [7] Clough RW, Ghanaat Y, Qiu X (1987) Dynamic reservoir interaction with Monticello Dam. EERC Rep UCB/EERC-87/21, Univ California, Berkeley.
- [8] Sevim B, Altunişık AC, Bayraktar A (2013) Structural identification of concrete arch dams by ambient vibration tests. Adv Concr Constr 1(3):227–237.
- [9] Tarinejad R, Ahmadi MT, Harichandran RS (2014) Full-scale experimental modal analysis of an arch dam: the first experience in Iran. Soil Dyn Earthq Eng 61–62:188–196.
- [10] Tarinejad R, Falsafian K, Aalami MT, Ahmadi MT (2016) Modal identification of Karun IV arch dam based on ambient vibration tests and seismic responses. J Vibroeng 18(6):3869–3880.
- [11] Proulx J, Paultre P, Rheault J, Robert Y (2001) An experimental investigation of water level effects on the dynamic behaviour of a large arch dam. Earthq Eng Struct Dyn 30(8):1147–1166.
- [12] Pereira S, Magalhães F, Cunha Á, Moutinho C, Pacheco J (2021) Modal identification of concrete dams under natural excitation. J Civil Struct Health Monit 11:465–484.
- [13] Darbre GR, Proulx J (2002) Continuous ambient-vibration monitoring of the arch dam of Mauvoisin. Earthq Eng Struct Dyn 31(2):475–480.
- [14] Pereira S, Reynders E, Magalhães F, Cunha Á, Gomes J (2019) Tracking the modal parameters of Baixo Sabor concrete arch dam with uncertainty quantification. In: Proc 2nd Int Conf on Uncertainty Quantification in Computational Sciences and Engineering, Crete, Greece, pp 24–26.
- [15] Wang JT (2011) Investigation of damping in arch dam-water-foundation rock system of Mauvoisin arch dam. Soil Dyn Earthq Eng 31(1):33–44.
- [16] Wu Y, Kang F, Wan G, Li H (2025) Automatic operational modal analysis for concrete arch dams integrating improved stabilization diagram with hybrid clustering algorithm. Mech Syst Signal Process 224:112011.

[17] Tarinejad R, Pourgholi M (2018) Modal identification of arch dams using balanced stochastic subspace identification. J Vib Control 24(10):2030–2044.

- [18] Pourgholi M, Tarinejad R, Khabir ME, Mohammadzadeh Gilarlue M (2023) System identification of Karun IV Dam using balanced stochastic subspace algorithm considering the uncertainty of results. J Vib Control 29(23–24):5342–5356.
- [19] Kalkan Okur E (2024) Determination of Structural Behavior and Long-Term Structural Health Monitoring in Deriner and Yusufeli Arch Dams by Considering Structure–Water–Soil Interaction. PhD Dissertation, Karadeniz Technical University.
- [20] Cao Z, Kashiwayanagi M, Yoshida M, Asaka H (2020) Evaluation method of damping ratio using earthquake records and its application in dam engineering. In: Proc 17th World Conf on Earthquake Engineering (17WCEE), Sendai, Japan.
- [21] Chopra AK (2020) Dynamics of Structures: Theory and Applications to Earthquake Engineering, 5th ed. Pearson, Boston.
- [22] López-Aragón JA, Puchol V, Astiz MA (2024) Influence of the modal damping ratio calculation method in the analysis of dynamic events obtained in structural health monitoring of bridges. J Civil Struct Health Monit 14(5):1191–1213.